Chiral Asymmetry in the Angle-Resolved O and C $1s^{-1}$ Core Photoemissions of the *R* Enantiomer of Glycidol

Ivan Powis,[1,*] Chris J. Harding,[1,¶]
Silko Barth,[2,§] Sanjeev Joshi,[2,§] Volker Ulrich,[2,§] and Uwe Hergenhahn[2,§]

[1] *School of Chemistry, University of Nottingham, NG7 2RD Nottingham, UK.*
[2]*Max-Planck-Institut für Plasmaphysik, EURATOM Association, Boltzmannstraße 2, 85748 Garching, Germany*

Running Title: Chiral Asymmetry in Glycidol Core Photoemission

PACS: 33.60.+q, 33.55.+b, 33.15.Ry, 33.15.Bh, 33.80.Eh

[¶] Current Address: *Lehrstuhl für Physikalische Chemie 1, Technische Universität München, Lichtenbergstraße 4, 85748 Garching, Germany*

[§] Mail Address: *c/o BESSY mbH, Albert-Einstein-Str. 15, 12489 Berlin, Germany*

* Corresponding Author:

Email: Ivan.Powis@Nottingham.ac.uk

Fax: +44 115 9513562

Tel: +44 115 9513467

Abstract

We present the first measurements of a photoelectron circular dichroism in photoionization from O and 1*s* core levels of the R-enantiomer of glycidol ($C_3H_6O_2$) in the gas phase. This dichroism emerges from a forward-backward asymmetry in the angular distribution of electrons created on ionization with circularly polarised synchrotron radiation and is already fully present in the pure electric dipole approximation. Asymmetry factors obtained for the core levels in this study range up to a few percent, but it is likely that these values are limited by a failure to resolve photoemission from individual atomic sites. Theoretical modelling is provided to examine potential differences between these alternative atomic photoemission sites, and between different conformational structures of glycidol. The calculated chiral angular distribution parameters that support the circular dichroism display a much enhanced sensitivity to the molecular conformation compared to the conventional photoionization cross-section and the β-parameter. Likely conformer structures can be suggested after comparison with the experiment.

1. Introduction

Photoelectron Circular Dichroism (PECD) records the asymmetry in the angular distribution of photoelectrons emitted from randomly oriented, enantiomeric samples of a chiral molecule following photoionization by a beam of circularly polarized light (CPL) [1]. A forward-backward asymmetry relative to the propagation direction of the light is predicted, and since it should reverse direction when either the handedness of the molecular target or the helicity of the radiation is exchanged a dichroism signal can be measured from the difference in yield in a given direction obtained with left and right circular polarizations. Asymmetry factors that typically range from a few- to a few tens per cent are obtained in PECD, orders of magnitude greater than is usual in electronic absorption circular dichroism (CD) measurements. This can be understood because PECD asymmetry is already present at the level of the pure electric dipole approximation, unlike CD which requires contributions from much weaker higher order terms (magnetic dipole, electric quadrupole) in the radiation-matter interaction. The forward-backward asymmetry will, however, cancel out in a non-angle resolving measurement, with the loss of much information concerning the molecular structure.

Initially, both computational[2-4] and experimental investigations[5-8] of the new PECD technique were focussed upon valence shell photoionization processes. But following on from these studies, C 1*s* core ionization has been investigated in a number of carbonyl containing molecules [9-12]. The large shift in binding energy of the **C**=O 1*s* electron means that it is readily resolved, allowing ionization from a single atomic site in the molecule to be experimentally recorded. Intuitively, it may seem probable that such an ionization, occurring from a spherical (and therefore achiral) initial orbital that is localised at a site other than the stereogenic centre, would lead to only weak sensitivity to the handedness of the host molecular frame. Indeed much routine application of X-ray photoelectron spectrometry (XPS) is founded on the premise that it is less a *molecular* spectroscopy, more an *atomic* element sensitive one. While molecule induced core binding energy shifts allow the presence of various functional groupings to be inferred, it is hardly classed as a sensitive tool for molecular structure determination.

Despite such misgivings it has been found that **C**=O 1*s* PECD does produce asymmetry factors that are at least as large as, arguably larger than, those encountered in valence shell

ionization of the same molecules [7, 9, 13, 14]. A key inference made from these observations is that the final state scattering of the outgoing photoelectron off the chiral molecular potential provides for an electron angular distribution that is very sensitive to the molecular structure, including its handedness, regardless of any chirality inherent to the initially ionized orbital.

The possibility for probing gas-phase molecular structure by examining the angle dependent final state electron scattering following site-specific core photoemission has been realised previously in the ionization of fixed-in-space CO molecules [15], while for surface adsorbed species such in-situ photoelectron diffraction studies are well established [16]. For a chiral species, PECD may similarly be capable of generating structural information, exploiting analogous electron scattering phenomena, but now achievable for isolated, randomly oriented molecules.

The carbonyl group plays a special role in conventional electronic circular dichroism measurements as a chromophore that provides enhanced CD signals due to the importance of the higher order contributions to the weak (nominally electric dipole forbidden) n-π^* transition moment. Such considerations ought not to apply to the PECD effect, which relies solely on the (fully allowed) electric dipole matrix elements for promotion of an electron into the ionization continuum; nevertheless it is now of interest to investigate core level ionizations other than that of the **C**=O 1*s* orbital to establish the generality and behaviour of the core electron PECD phenomenon.

In this paper we present the first observations of core electron PECD not made at the carbon K-edge, and further examine C 1*s* PECD from sites other than carbonyl groups. We have chosen to examine ionizations of the chiral molecule glycidol ($C_3H_6O_2$). Glycidol contains two O atoms, one in its epoxy ring (which we hereafter designate O_R) and one in the hydroxyl group (designated O_H). Initially, it was hoped that these would have different binding energies, allowing ionization at two different sites in the same molecule to be examined. Unfortunately, it was found that the XPS in the O K-edge region displays a single band, meaning that the O_H $1s^{-1}$ and O_R $1s^{-1}$ ionizations are fully overlapped and not resolvable, but the behaviour of the composite O $1s^{-1}$ peak has been examined both experimentally and theoretically. Similarly, measurements made from glycidol's three overlapping C $1s^{-1}$ emissions are described.

Full theoretical analyses of these composite PECD photoemissions are provided using multiple-scattering model calculations. These examine the markedly varying contributions from a number of theoretically predicted, low energy conformations. Comparison with the experimental data then corroborates previous complementary experimental data identifying the two most populated structures present in a thermal sample. The multiple-scattering photoionization dynamics calculations also examine the predicted PECD contributions from individual localised atomic sites. A greatly enhanced sensitivity of the purely chiral scattering terms to small changes in molecular structure and photoemission site is revealed.

2. Experimental Method

The core ionization spectra were recorded using the soft X-ray UE56/2 beamline at the BESSY synchrotron. Measurements were made using a conventional hemispherical analyzer with a multichannel detector (Scienta ES 200) mounted at 54.7° with respect to the light beam direction, and the dichroism was recorded using this fixed detection angle in conjunction with rapid polarization switching of the twin undulator source [17]. These

measurements utilised the analyser's fixed window mode so that complete spectra were recorded at each 0.1 Hz polarization switch. Considerable efforts are made to follow procedures that ensure comparability between irradiation with either undulator and polarization combination and hence effectively cancel any instrumental asymmetry. Full details of this methodology, the apparatus, and the data reduction techniques employed are given elsewhere [10].

The experimental PECD asymmetry factor is defined as the normalised difference between the background corrected spectra, S_p recorded with left and right CPL (respective helicities $p = +1$, $p = -1$):

$$\Gamma_{54.7} = \left(S_{+1} - S_{-1}\right) \Big/ \left(\left(S_{+1} + S_{-1}\right)/2\right).$$

Equation 1

It is assumed that the angle resolved spectra can be expressed in terms of a total ionization rate and a normalized angular distribution function, $I_p(\theta)$, hence $S_p = N_p I_p(\theta)$. An aim of the experimental methodology [10] is to ensure that the total rates, N_p , are set, or otherwise compensated, so as to be equal, i.e. $N_{+1} = N_{-1}$. The experimental asymmetry factor, determined by the application of Equation 1, can thus be re-written and interpreted in terms of the angular distribution function:

$$\Gamma(\theta) = \left(I_{+1}(\theta) - I_{-1}(\theta)\right) \Big/ \left(\left(I_{+1}(\theta) + I_{-1}(\theta)\right)/2\right).$$

Equation 2

The expected form of the angular distribution obtained with pure polarization of the ionizing radiation, in the electric dipole approximation, is [3, 18] :

$$I_p(\theta) = 1 + b_1^p P_1(\cos\theta) + b_2^p P_2(\cos\theta),$$

Equation 3

where P_n is the n^{th} order Legendre polynomial and the coefficients b_n^p depend on the photoionization dynamics as well as on the photon helicity, p. Only for the very particular case of circularly polarized radiation ($p = \pm 1$) and a chiral target molecule is the parameter b_1^p *a priori* non-zero. Then, however, it leads to a forward-backward asymmetry in the electron angular distribution around the light propagation direction, since the $P_1(\cos\theta) = \cos\theta$ term is odd with respect to the exchange $\theta \leftrightarrow (\pi - \theta)$.

Taking advantage of the antisymmetry of the P_1 coefficients [3, 18], $b_1^{\{+1\}} = -b_1^{\{-1\}}$, and the symmetry of the P_2 coefficients, $b_2^{\{+1\}} = b_2^{\{-1\}} \left(= -\frac{1}{2}\beta\right)$, Equation 3 may be substituted into Equation 2 yielding

$$\Gamma(\theta) = 2b_1^{\{+1\}} P_1(\cos\theta) \Big/ 1 + b_2^{\{\pm 1\}} P_2(\cos\theta).$$

Equation 4

For our specific choice of the so-called magic angle, θ = 54.7°, the P_2 polynomial has a value of zero so that writing the remaining P_1 polynomial explicitly one obtains:

$$\Gamma(54.7) = 2b_1^{\{+1\}} \cos 54.7$$

Equation 5

A parallel argument can be advanced to demonstrate that the forward-backward asymmetry seen between emission at 0° and 180° with a fixed CPL state, implied by the angular distribution in Equation 3, may also be expressed as [14] :

$$G_{AD} = 2b_1^{\{+1\}} .$$

Equation 6

Comparing the experimental dichroism, $\Gamma_{54.7}$ (Equation 1), with the predicted form, Equation 5, allows the $b_1^{\{+1\}}$ parameter to be estimated and compared with theoretical predictions. Similarly, either this estimate or a calculation for the chiral coefficient permits the forward-backward angular asymmetry factor, G_{AD}, to be readily predicted.

R-(+) glycidol (Sigma-Aldrich) with a stated purity of 97 % was used without further purification in a gently heated inlet system. The sample vapour was admitted via a control valve to the ionization source, a gas cell that was heated to 5 — 10 °C above ambient temperature to minimise condensation of the sample vapour around the spectrometer inlet. Estimated pressures in this cell during measurements are ~5×10^{-5} mbar, and this results in a sample consumption of ~20 mg h^{-1}.

3. Computational details

Photoionization electric dipole matrix elements were calculated using a continuum multiple scattering method (CMS-Xα). Our procedure for this has been described previously [19-21]. In particular, we here follow closely the parameterizations adopted in a recent study of the valence shell PECD of glycidol [22]. In that work, the basis set of spherical harmonic functions used to calculate the self-consistent neutral molecule potential was truncated at l_{max}= 3 at the C and O atom centres, and at l_{max}= 0 on the H atoms. For the asymptotic region l_{max}= 7. This minimal basis for the H atom centres was shown to be insufficient when H-bonding interactions strongly polarise the H atom functions in the orbital to be ionized [22].While this is not a direct concern for the core level calculations, other recent work has shown that such polarization of the molecular electron density can be significant in the scattering of the emitted electron coming from any initial orbital [23]. Consequently, the neutral molecule calculations were here extended with l_{max}= 1 on all the H atoms. This neutral molecule basis set ($l_{max} = 7,3,1$) was increased to $l_{max} = 18,10,8$ (the asymptotic, C/O atom, and H atom regions respectively) for the continuum electron function calculations, as before [22]. With continuum functions available, electric dipole photoionization matrix elements are calculated and then are used to obtain photoionization cross-sections and the angular distribution parameters appearing in Equation 3 [3, 18].

4. Results and Discussion

Survey spectra using the R-enantiomer of glycidol were recorded just above the C and O K-edges; a single photoelectron peak was identified in each region. More extended measurements were then made for each of these peaks to observe the PECD.

Figure 1 shows the single O $1s^{-1}$ XPS band recorded with CPL at a photon energy of 543 eV. The difference in intensity between the bands recorded with oppositely polarized

CPL under conditions that are constrained by our experimental procedures to be otherwise effectively identical [10] is clearly seen. The resulting experimental asymmetry, $\Gamma_{54.7}$, obtained channel by channel across the peak is plotted on the same figure. Within the estimated statistical uncertainty represented by the error bars the asymmetry remains reasonably flat across the FWHM of the photoelectron peak, and for convenience in the following discussion we consider the mean value of $\Gamma_{54.7}$ across the FWHM, which is -0.026 ± 0.002 .

In this wavelength region the radiation is generated as the undulator third harmonic, and consequently the polarization is elliptical rather than purely circular. This polarization state is defined using the Stokes parameters, s_i, that are related as $1 = \sqrt{{s_1}^2 + {s_2}^2 + {s_3}^2} + s_4$. The azimuthal detector angle ϕ is measured from the direction aligned with the $s_1 = +1$ horizontal linear polarization component. In the present circumstances it can be assumed that the undulator radiation is fully polarized ($s_4 = 0$) and also that $s_2 = 0$ [17, 24]. The expected angular distribution Equation 3 has then to be modified [25]:

$$I'_{\pm 1}(\theta,\phi) = 1 + |s_3| b_1^{\{\pm 1\}} P_1(\cos\theta) + b_2^{\{\pm 1\}} \left[P_2(\cos\theta) + \tfrac{3}{2}\left(s_1 \cos 2\phi + s_2 \sin 2\phi\right)\sin^2\theta \right],$$

Equation 7

Substituting Equation 7 into Equation 2 with the appropriate detector angles ($\theta = 54.7°$, $\phi = 90°$) and simplifying we obtain:

$$\Gamma'(54.7) = \frac{2}{\sqrt{3}} |s_3| b_1^{\{+1\}} \Big/ \left(1 + b_2^{\{\pm 1\}} s_1\right) = \frac{2}{\sqrt{3}} |s_3| b_1^{\{+1\}} \Big/ \left(1 - \tfrac{1}{2}\beta s_1\right),$$

Equation 8

Both Equation 7 and Equation 8 are readily seen to reduce to, respectively, Equation 3 and Equation 5 for the case of pure circular polarization ($s_3 = \pm 1,\ s_1 = s_2 = 0$). At 543 eV the estimated beamline circular polarization is $s_3 = \pm 0.895$ and consequently $s_1 = \sqrt{1 - {s_3}^2} = 0.446$ (i.e. a polarization ellipse with horizontal principal axis). By equating the experimental asymmetry measure, $\Gamma_{54.7}$ (Equation 1) with Equation 8 and rearranging, an estimate for the R-enantiomer chiral angular distribution parameter, $b_1^{\{+1\}}$, can be obtained. However, because $s_1 \neq 0$ this polarization correction requires that a value for β be assumed.

The current experimental configuration does not permit an independent determination of β to be attempted. A priori, one might plausibly expect that a few eV above threshold, as here, β would fall somewhere in the range 0 to +1.0 . Lacking any further information we will assume $\beta = 0.5 \pm 0.5$ and so arrive at a polarization corrected estimate for $b_1^{\{+1\}}$, incorporating the stated uncertainty in β, of -0.022 ± 0.003. This figure is equivalent to an overall chiral asymmetry in the forward-backward photoemission, G_{AD} = 4.4%.

A comparison with theory has to start with the recognition that glycidol has potentially nine possible conformers from rotation around the C—OH and C—CH_2OH bonds. These have been studied at various levels of theory [22, 26, 27]. In Figure 2 we show the six lowest energy conformers and in Table 1 we summarise our own Gaussian-2 calculations[28] and the resulting population estimates. These calculations, microwave spectroscopy[27] at –10 C°, Fourier Transform Infrared spectroscopy in a cold jet, and valence region PECD

measurements[22] made using a supersonic molecular beam all conclude that the intramolecular H-bond stabilised conformers, **C1** and to a lesser extent **C2**, comprise the majority species present, with no definitive evidence for a population of **C3** or above.

CMS-Xα calculations giving the combined O_R and O_H $1s^{-1}$ cross-sections and the cross-section weighted averaged β-parameters for each of the conformers **C1** — **C5** are shown in Figure 3. There is evidently little variation with conformer in either the expected cross-section or, with the possible exception of **C1**, in the expected β-parameter. The calculated β parameters do, however, offer support for the assumption made above when correcting the experimental chiral asymmetry, that β = 0.5 in the region approximately 5 eV above threshold, whichever of these conformers might be involved.

In Figure 4 we proceed to compare the corresponding calculated chiral b_1^{+1} parameters for R-enantiomer conformers **C1**—**C5** and also include the experimental O $1s^{-1}$ datum. Unfortunately, post-experimental data analysis revealed some unexpected drift in the electron energy scale between various calibration scans. The use of rapid polarization switching during dichroism measurements automatically guards against adverse effects from a slow drift, and in fact detailed examination of the data readily verifies that there is no discernible drift for either polarization setting/undulator during the course of a single complete PECD measurement run. However this long-term drift, together with the finite XPS peak width, contributes to the indicated energy uncertainty of the datum in Figure 4. The calculated curves are again generated as cross-section weighted averages of the two O atom site ionizations. The uncertainties occasioned by this averaging and the limited data notwithstanding, only the **C1** and (improbable) **C5** conformers have predicted values that are close to agreement in magnitude, and even sign, with the experimental result at 4.8 eV kinetic energy. From Table 1 the estimated population ratio at the approximate temperature of our experiment (298 K) is 2:1 **C1**:**C2** using calculated free energies (3.5:1 using temperature corrected internal energies) with less than 10 % population of other conformers. Comparison of the mean O_H/O_R calculations with the single experimental value available here could never provide a definitive conclusion, but nevertheless the 2:1 weighted average of the **C1** and **C2** predicted $b_1^{\{+1\}}$ parameter at 4.8 eV is –0.020 so matching the experimental value. A thermal sample comprising a major **C1** component, a minor **C2** component and essentially negligible amounts of other possible conformers is thus plausible given the data assembled in Figure 4 and is consistent with the other available data described above [22, 26, 27].

One of the more fascinating aspects of the calculated PECD is the great variation between individual conformers that is revealed in Figure 4. This contrasts greatly with the near identical cross-section and β parameter behaviour from the same calculations that is evident in Figure 3. Although they may be of only limited experimental significance given the sample conditions in this work, it is particularly interesting to examine the PECD behaviour predicted for conformers **C3**, **C4**, and **C5**. From Figure 2 it can be seen that these three differ only in the dihedral angle formed by the –OH group; everything in the rest of the molecule is essentially fixed while the hydroxyl H atom adopts different positions. Yet despite these seemingly limited structural variations, the expected PECD changes dramatically in each conformer; this is most clearly seen around 5 eV in Figure 4.

To better understand this it seems worthwhile to examine the individual O_H and O_R $1s^{-1}$ $b_1^{\{+1\}}$ parameter curves, even though it has not been possible experimentally to resolve their contributions. Figure 5 presents the calculated PECD associated with each individual O atomic site. Focussing particularly on the region around 5 eV kinetic energy, it can be seen

that PECD results from the ring atom site, O_R, are very similar for the three conformers **C3**—**C5**, but that the O_H PECD results show very striking differences. This is much as might be intuitively expected, since the latter photoemission site is immediately adjacent to where the major structure changes occur. For reasons that are not so intuitive the converse behaviour appears for the **C1** and **C2** conformers, where at ~5 eV it is the ring O_R site that responds greatly to the changes in molecular structure.

Turning now to the carbon K edge, typical XPS results for the two circular polarization states, and the deduced asymmetry between them are presented in Figure 6. Again there is some residual uncertainty (±1 eV) in the indicated electron energy scale, due to the drift noted between preliminary and final calibration runs. Only a single XPS peak is observed, the three individual C atom contributions being strongly overlapped. In contrast to the O1*s* spectra of Figure 1 there are clear indications at several photon energies that a significant variation of the asymmetry occurs across the width of the peak. One can speculate that this results from varying contributions made by the individual core orbitals as their degree of overlap changes across the observed effective peak shape. Nevertheless, given the uncertainty in such component peak overlap no attempt is made to model this behaviour more closely, and instead we continue to deal with mean asymmetry values that are derived from across the experimental peak FWHM. As for the oxygen edge, $b_1^{\{+1\}}$ parameter values are inferred from the mean asymmetry, $\Gamma_{54.7}$, after allowance for the cos 54.7° term. Radiation at the C edge is generated as the first undulator harmonic, and the measured polarization rates are near to 100 %, so that here no explicit polarization correction is required [10]. The results are plotted in Figure 7 along with the CMS-Xα calculations for conformers **C1** —**C5**, each of these curves being an average of the three C atom asymmetries weighted by the calculated cross-sections.

As before, it is interesting to note the significant variations in the predicted PECD shown by the different conformations of glycidol. Forewarned with the expectation from previous work[22, 26, 27] and the calculations in Table 1 that the **C1** (**C2**) conformers will dominate in the experimental sample, it can be appreciated that the calculated curves for these two appear in closest agreement with experiment. That the quality of the theory-experiment match isn't more striking is perhaps inevitable given the quantitative uncertainty associated with the weightings required for a fully realistic averaging of the three atomic site contributions in the two conformers that we infer are populated.

However, there is once more some interest in examining the predicted PECD before the averaging necessary to facilitate comparison with experiment. Figure 8 shows these curves for each of the individual C atomic sites. First, it can be noted that while the typical PECD asymmetry predicted at the central asymmetric carbon at low kinetic energies is typically of slightly greater magnitude than for the other C site in the oxirane ring, there is no significant difference in magnitude when photoemission from this chiral C atom is compared with that at the other C atom site, in the **C**H_2OH grouping. So photoemission localised at the stereogenic centre does not lead, *per se*, to strong enhancement of the chiral asymmetry expected in the photoelectron angular distribution. This underlines once more that the photoelectron senses the molecular chirality as a final state effect as it is scattered off the non-local chiral potential; given the achiral nature of a spherical 1*s* orbital there is here emphatically no initial state chiral commitment of the ionized electron.

Second, while at both the chiral- and methanolic-C atom sites the **C1** and **C2** conformer calculations predict very different behaviour, the related **C3** — **C5** conformers (which we include for interest more than as expected contributors to the experimental result) are quite similar to one another. To some degree, the converse is true at the second ring C atom site.

Third, it is also clear from an examination of Figure 7 and Figure 8 that the PECD asymmetry predicted from individual orbitals may typically exceed that obtained from unresolved bands. The averaging implied in the latter case inevitably reduces any individually large contributions towards a much smaller mean; this is especially true since the expected bipolar character of the $b_1^{\{+1\}}$ parameters means that two contributions of similarly large magnitude, but opposite sign, may effectively cancel to zero.

5. Conclusions

We have presented the first O $1s^{-1}$ Photoelectron Circular Dichroism (PECD) measurement, as well as several C $1s^{-1}$ PECD measurements made above the carbon K-edge for the R-enantiomer of the oxirane derivative glycidol. Unfortunately, neither the individual O atom sites, nor the individual C atom sites proved to be resolvable since the O and C binding energy shifts were found to be essentially the same in each atom type. The PECD asymmetry factors recorded were smaller than have been previously measured for carbonyl **C**=O $1s^{-1}$ photoemission, but the calculations made for the individual orbital ionizations suggest that any comparative reduction in the magnitude of the PECD may be more a consequence of the averaging over unresolved orbital contributions, tending towards a lower net PECD asymmetry, than indicators of any intrinsic weakness in the new categories studied here. Even so, with values of a few per cent these core level asymmetry factors are still significantly larger than other typical chiroptical asymmetries. These results also confirm that PECD may be expected to arise in any core level photoemission in a chiral molecule, and being present in the electric dipole approximation PECD is not necessarily restricted to certain special chromophores or atomic photoemission sites.

The behaviour calculated indicates how, under some circumstances, the PECD can be expected to be extremely sensitive to molecular conformation, even to simple changes in the dihedral angle of the single hydroxyl H atom. The asymmetry predicted from the central asymmetric C atom is not, however, especially enhanced relative to other photoemission sites. From this it is inferred that the significant influence of molecular chirality on the photoelectron angular distribution is exerted through a non-local final state scattering of the departing photoelectron off the chiral molecular ion potential.

Acknowledgments

This experimental work was supported by the European Community – Research Infrastructure Action. We are indebted to the technical general staff of BESSY for running the SR facility. The calculations benefited from helpful exchanges with Dr. Mauro Stener and by the provision of resources by the EPSRC National Service for Computational Chemistry Software.

Table 1 Gaussian-2 calculated energies and relative populations of glycidol conformers.

Conformer τ_1 τ_2 [a]	**G2MP2** [b]		**50 K**		**298 K**		**298 K**		**350 K**	
	(a.u.) [c]	**ΔE (kJ mol^{-1})**	**G (a.u.)** [c]	**Pop.**	**U (a.u.)**	**Pop.**	**G (a.u.)** [c]	**Pop.**	**G (a.u.)** [c]	**Pop.**
g^+g^- (**C1**)	-267.893890		-267.897217	99.7 %	-267.888674	73.1 %	-267.921893	58.4 %	-267.927977	51.3 %
g^-g^+ (**C2**)	-267.892938	2.5	-267.896208	0.3 %	-267.887561	22.5 %	-267.921343	32.6 %	-267.927526	34.2 %
g^+a (**C3**)	-267.890764	8.2	-267.894112	0 %	-267.885306	2.1 %	-267.919242	3.5 %	-267.925453	5.3 %
tt (**C4**)	-267.890304	9.4	-267.893652	0 %	-267.884752	1.1 %	-267.918932	2.5 %	-267.925186	4.1 %
g^-a (**C5**)	-267.889986	10.2	-267.893338	0 %	-267.884419	0.8 %	-267.918658	1.9 %	-267.924923	3.3 %
g^+g^+ (**C6**)	-267.889457	11.6	-267.892803	0 %	-267.883913	0.5 %	-267.918052	1.0%	-267.924300	1.9 %

[a] Conformation $\tau_1\tau_2$ defined following Borho and Suhm [26] identifying the H-O_H-C-C and O_H-C-C-O_R torsional angles respectively as either gauche or trans. Notice, however, that since we refer to the R-enantiomer the gauche sign convention is the opposite of theirs which referred instead to the S-enantiomer.
[b] Absolute electronic + zero point vibrational energy (0 K)
[c] These energies previously reported in Ref. [22] except for the *tt* conformer (C4).

Figures

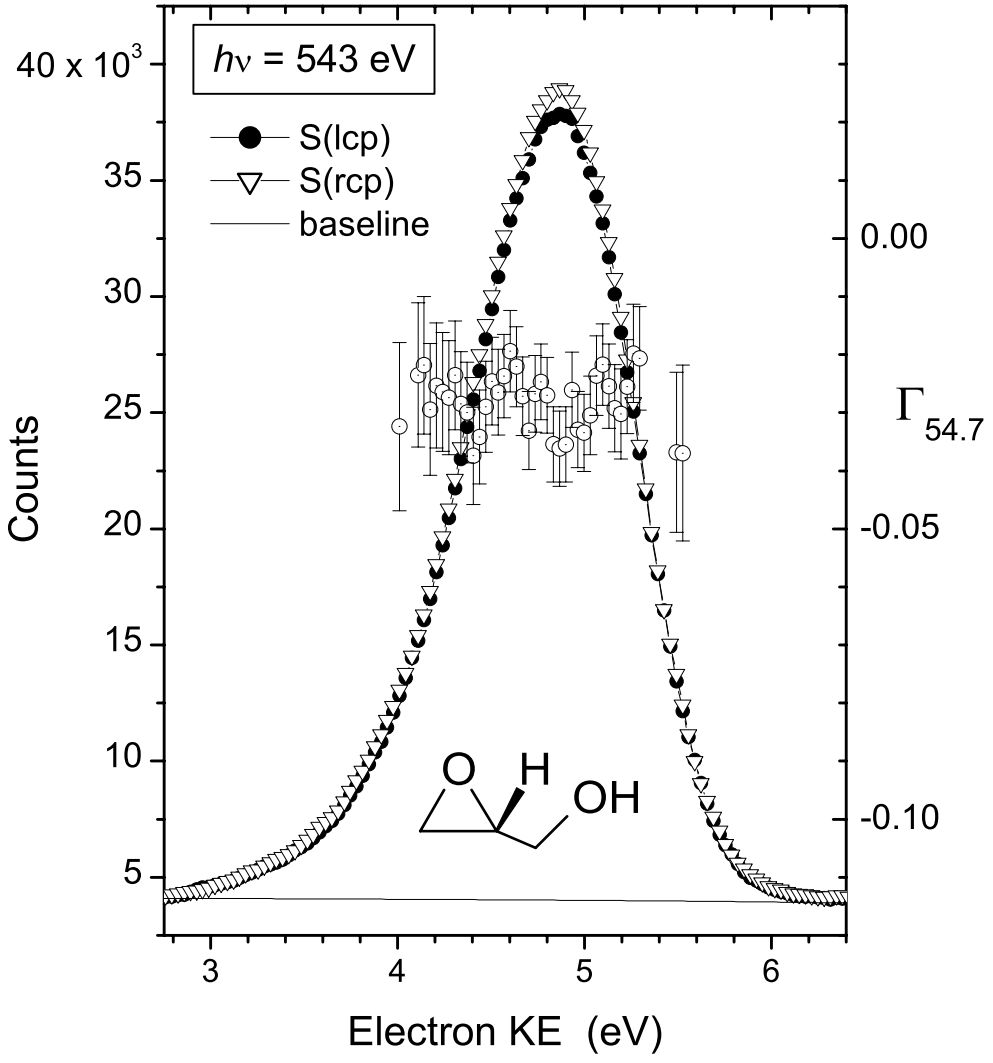

Figure 1 O 1*s* XPS of R-glycidol. Spectra, S(lcp) and S(rcp), recorded with left and right circularly polarised radiation are shown, together with $\Gamma_{54.7}$, the experimental asymmetry between them.

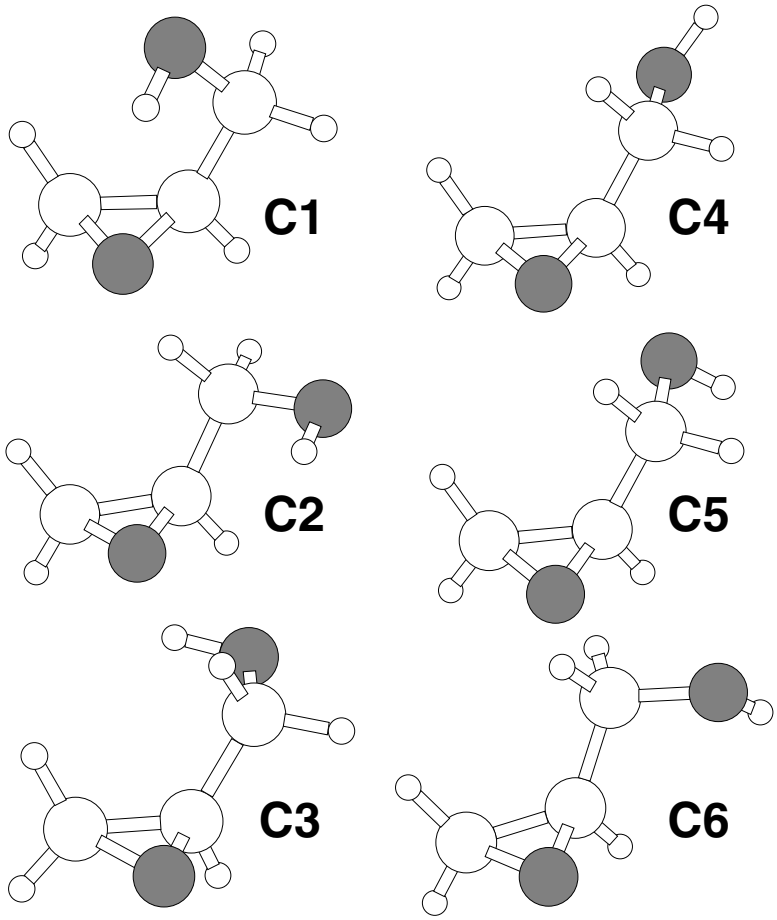

Figure 2 Lowest energy glycidol conformers. For greater clarity the oxygen atoms are drawn shaded.

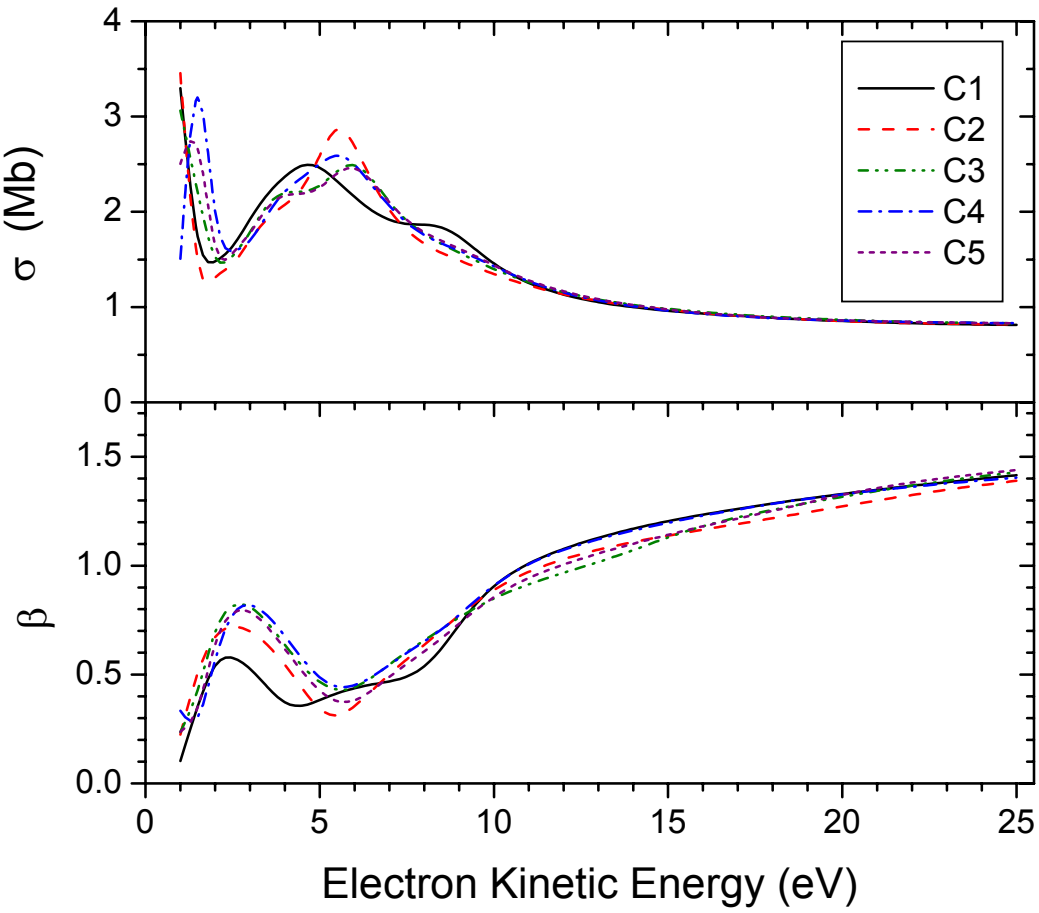

Figure 3 (color online) CMS-Xα O 1*s* photoionization calculations for glycidol conformers **C1** … **C5**. For each conformer the cross-section curves, σ, represent the sum of the O_R and O_H atom $1s^{-1}$ ionization, while the β anisotropy parameters are cross-section weighted averages for these two photoemission sites.

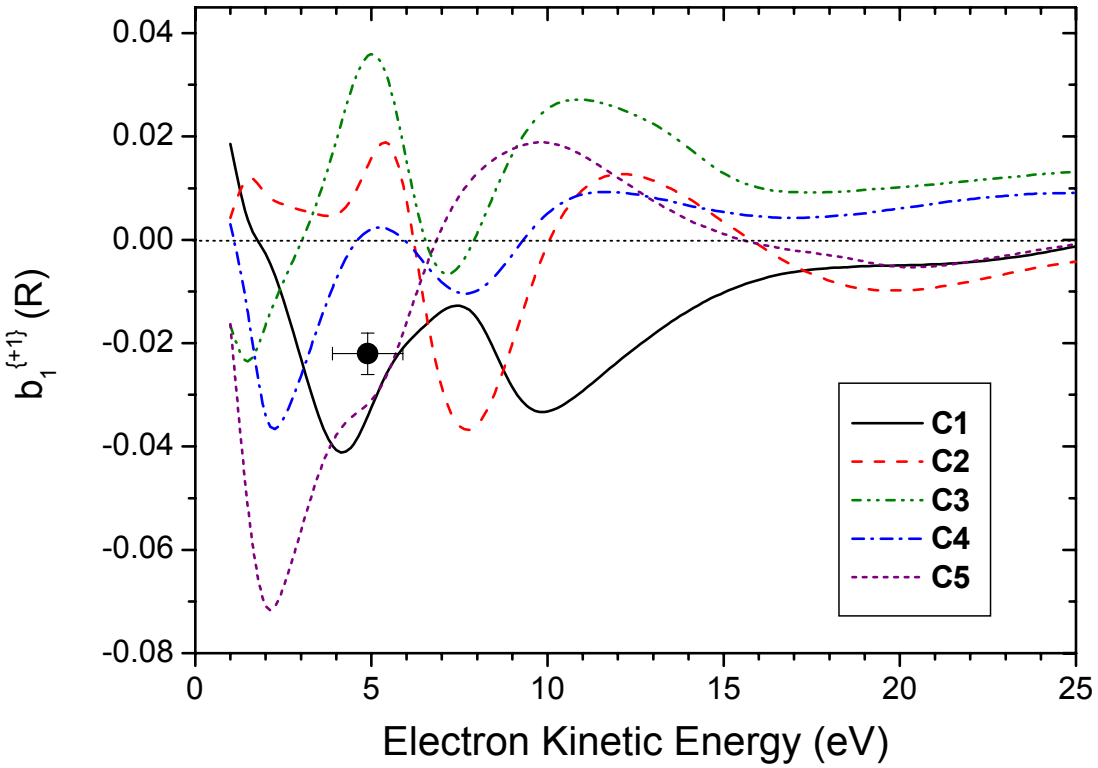

Figure 4 (color online) Calculated O 1s PECD curves for conformers of R-glycidol with experimental datum measured at $h\nu$ = 543 eV for comparison. Each conformer curve is a cross-section weighted average of the O_R and O_H atom photoemission.

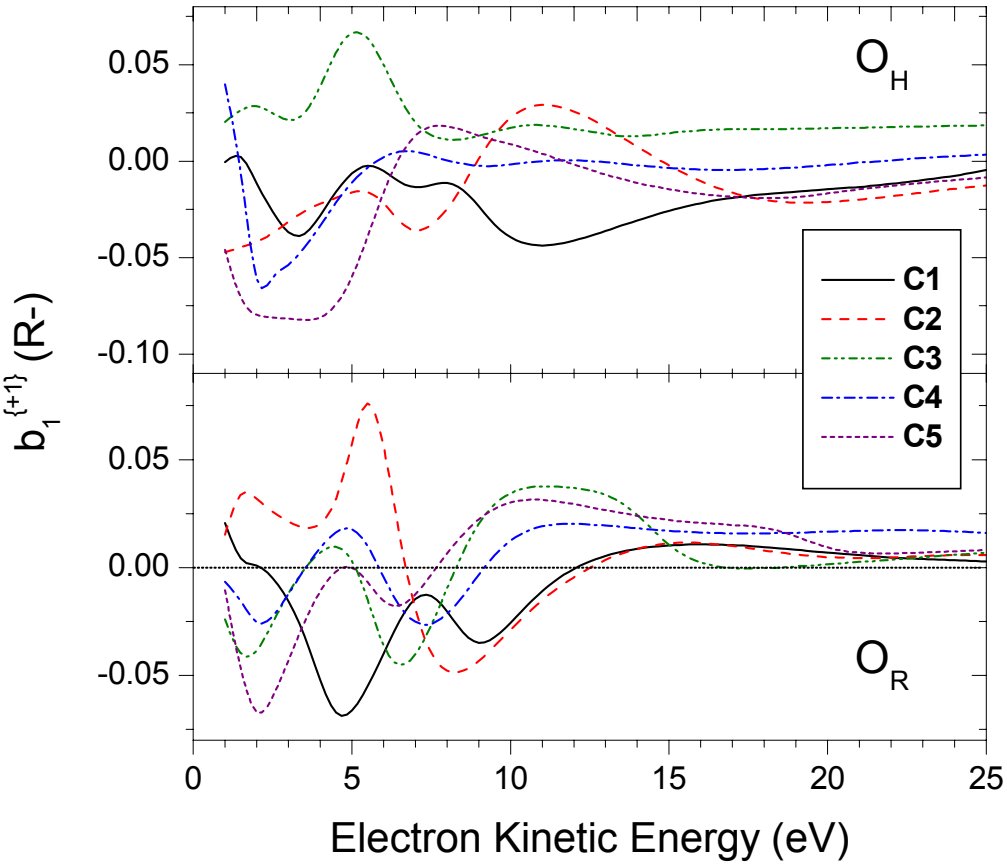

Figure 5 (color online) Calculated O atom $1s^{-1}$ $b_1^{\{+1\}}$ parameters for the conformers **C1** — **C5** of R-glycidol.

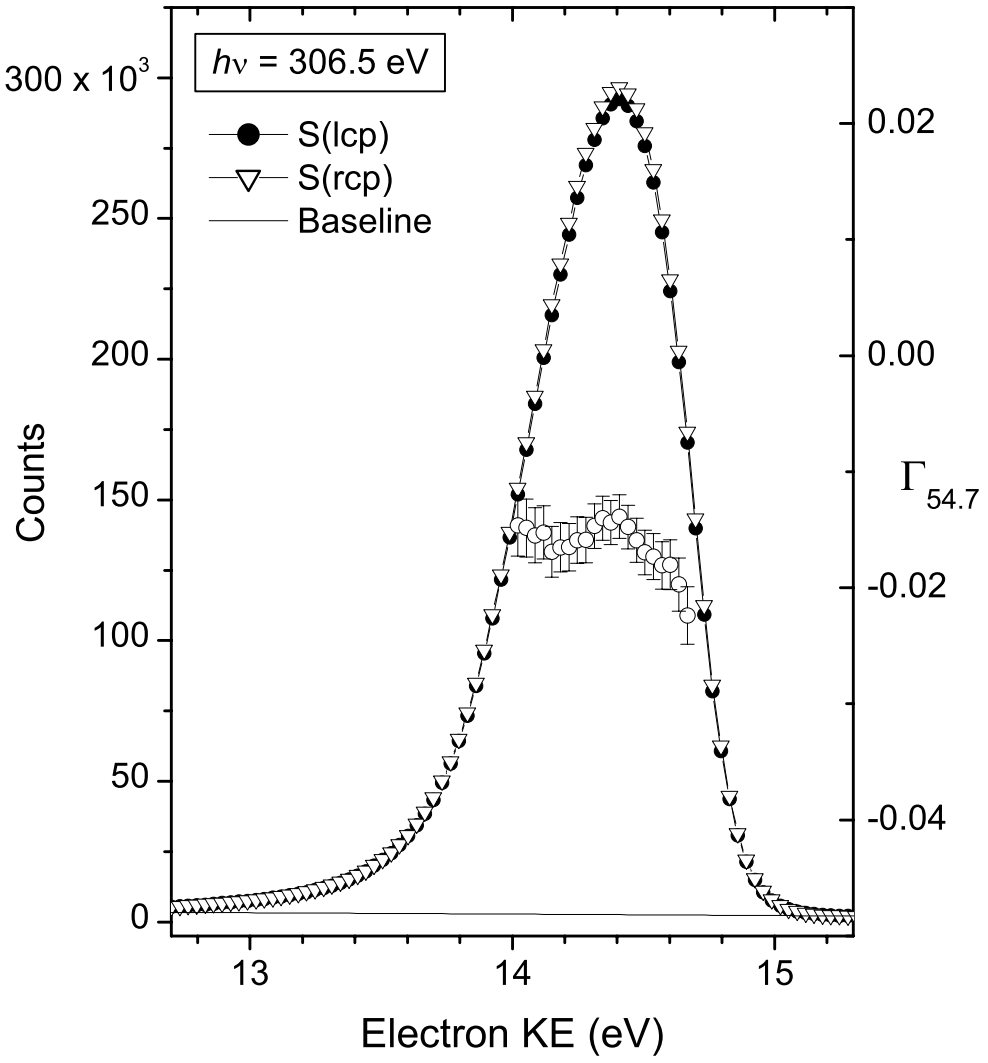

Figure 6 C 1s XPS of R-glycidol. Recorded spectra obtained using left and right circular polarization are shown, together with $\Gamma_{54.7}$, the experimental asymmetry between them.

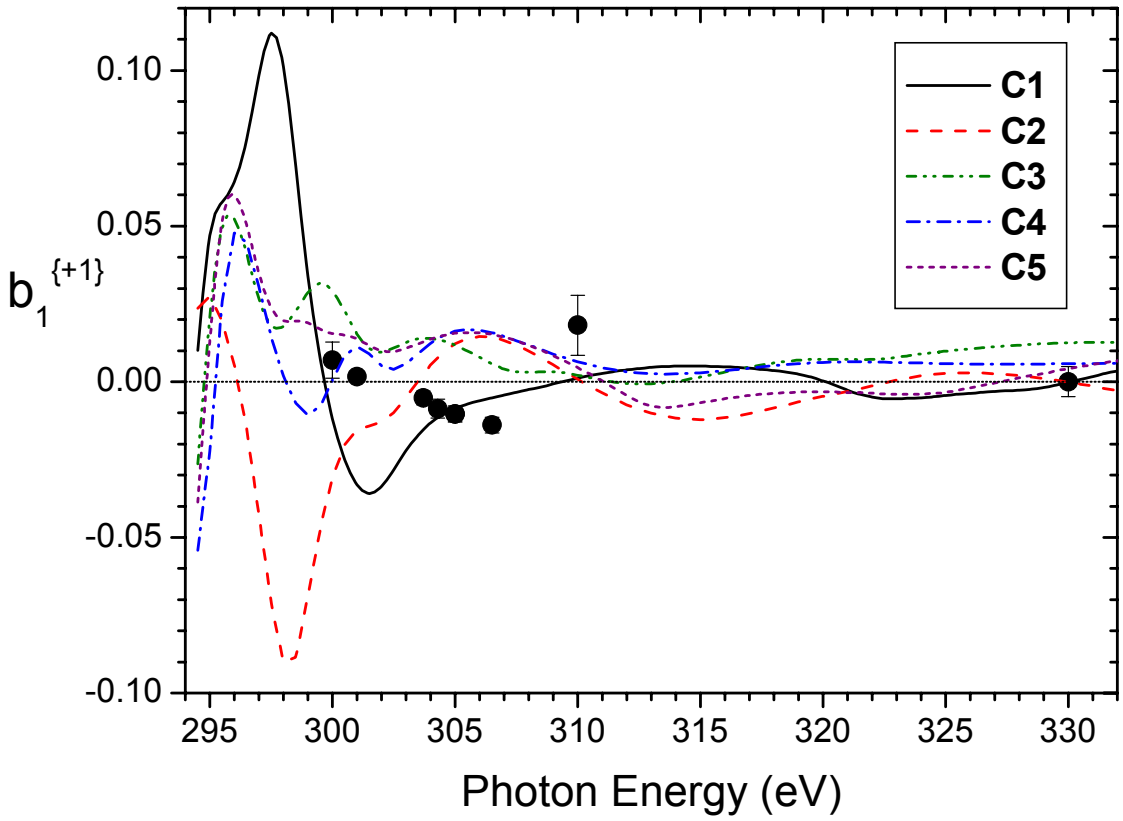

Figure 7 (color online) Experimental (●) and calculated C 1s PECD results for R-glycidol. Each calculated conformer curve **C1** — **C5** is a cross-section weighted average of the three C atom photoemission sites within the molecule.

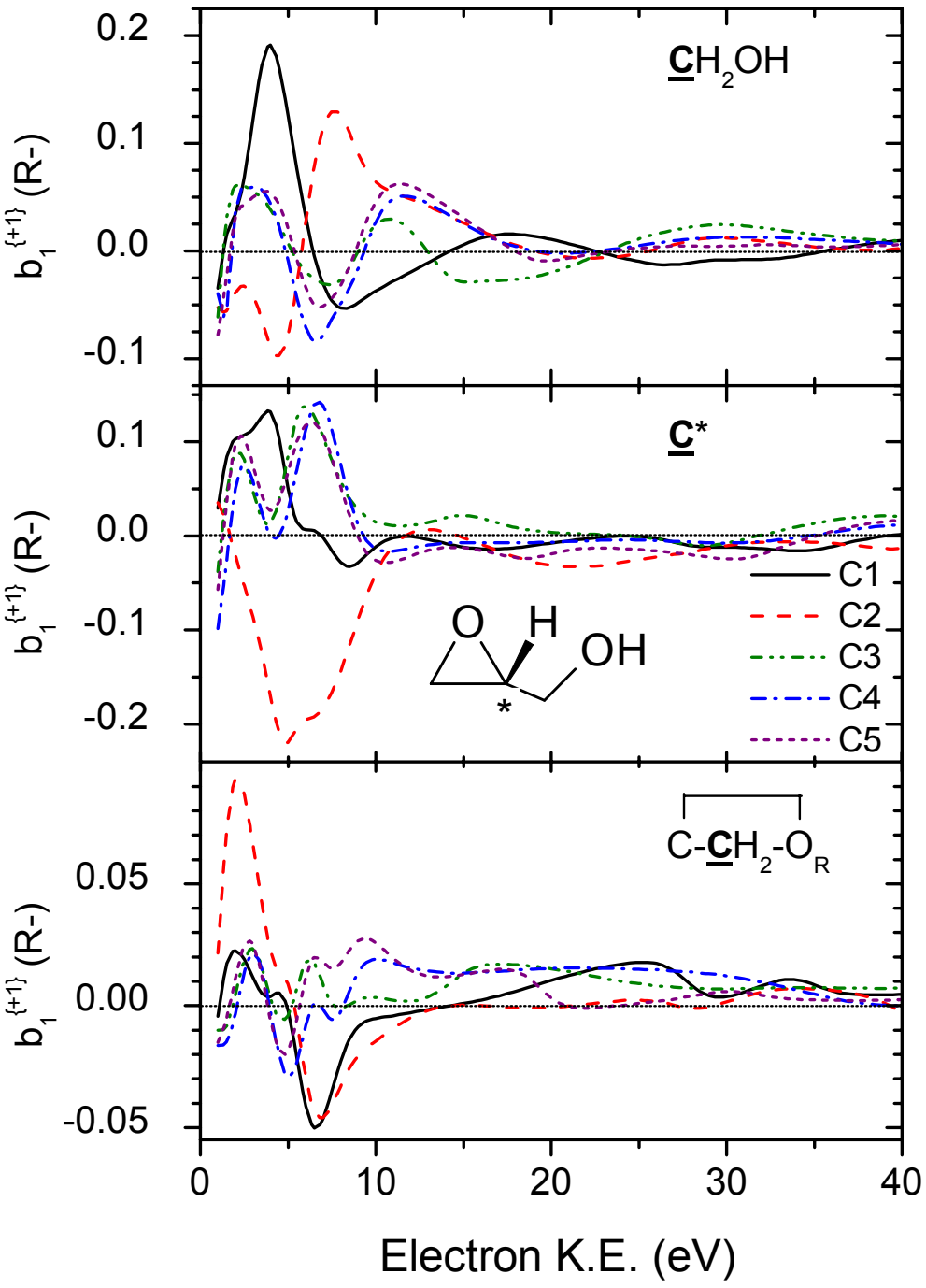

Figure 8 (color online) Calculated C atom $1s^{-1}$ $b_1^{\{+1\}}$ parameters for the conformers **C1** — **C5** of R-glycidol: methanolic C (upper panel); stereogenic (chiral) C (middle panel); second oxirane ring C (lower panel).

References

[1] I. Powis, in *Advances in Chemical Physics*, edited by J. C. Light (Wiley, New York, 2008), Vol. 138, p. 267.
[2] I. Powis, J. Phys. Chem. A **104**, 878 (2000).
[3] I. Powis, J. Chem. Phys. **112**, 301 (2000).
[4] M. Stener, G. Fronzoni, D. Di Tommaso, and P. Decleva, J. Chem. Phys. **120**, 3284 (2004).
[5] N. Böwering, T. Lischke, B. Schmidtke, N. Müller, T. Khalil, and U. Heinzmann, Phys. Rev. Lett. **86**, 1187 (2001).
[6] G. A. Garcia, L. Nahon, M. Lebech, J. C. Houver, D. Dowek, and I. Powis, J. Chem. Phys. **119**, 8781 (2003).
[7] T. Lischke, N. Böwering, B. Schmidtke, N. Müller, T. Khalil, and U. Heinzmann, Phys. Rev. A **70**, art. no.022507 (2004).
[8] S. Turchini, N. Zema, G. Contini, et al., Phys. Rev. A **70**, art. no.014502 (2004).
[9] U. Hergenhahn, E. E. Rennie, O. Kugeler, S. Marburger, T. Lischke, I. Powis, and G. Garcia, J. Chem. Phys. **120**, 4553 (2004).
[10] C. J. Harding, E. A. Mikajlo, I. Powis, S. Barth, S. Joshi, V. Ulrich, and U. Hergenhahn, J. Chem. Phys. **123**, 234310 (2005).
[11] C. J. Harding and I. Powis, J. Chem. Phys. **125**, 234306 (2006).
[12] V. Ulrich, S. Barth, S. Joshi, U. Hergenhahn, E. A. Mikajlo, C. J. Harding, and I. Powis, J. Phys. Chem. A **112**, 3544 (2008).
[13] C. J. Harding, Ph.D. thesis, Nottingham University, 2005.
[14] L. Nahon, G. A. Garcia, C. J. Harding, E. A. Mikajlo, and I. Powis, J. Chem. Phys. **125**, 114309 (2006).
[15] A. Landers, T. Weber, I. Ali, et al., Phys. Rev. Lett. **87**, 013002 (2001).
[16] D. P. Woodruff and A. M. Bradshaw, Rep. Prog. Phys. **57**, 1029 (1994).
[17] M. R. Weiss, R. Follath, K. J. S. Sawhney, et al., Nucl. Instrum. Methods Phys. Res. A **467**, 449 (2001).
[18] B. Ritchie, Phys. Rev. A **13**, 1411 (1976).
[19] I. Powis, Chem. Phys. **201**, 189 (1995).
[20] Y. Hikosaka, J. H. D. Eland, T. M. Watson, and I. Powis, J. Chem. Phys. **115**, 4593 (2001).
[21] P. Downie and I. Powis, J. Chem. Phys. **111**, 4535 (1999).
[22] G. A. Garcia, L. Nahon, C. J. Harding, and I. Powis, Phys. Chem. Chem. Phys. **10**, 1628 (2008).
[23] I. Powis, C. J. Harding, G. A. Garcia, and L. Nahon, ChemPhysChem **9**, 475 (2008).
[24] J. Bahrdt, W. Frentrup, A. Gaupp, M. Scheer, W. Gudat, G. Ingold, and S. Sasaki, Nucl. Instrum. Methods Phys. Res. A **467**, 21 (2001).
[25] K. N. Huang, Phys. Rev. A **22**, 223 (1980).
[26] N. Borho and M. A. Suhm, Phys. Chem. Chem. Phys. **4**, 2721 (2002).
[27] K. M. Marstokk, H. Mollendal, and Y. Stenstrom, Acta Chem. Scand. **46**, 432 (1992).
[28] L. A. Curtiss, K. Raghavachari, G. W. Trucks, and J. A. Pople, J. Chem. Phys. **94**, 7221 (1991).